JOURNAL OF MATERIALS SCIENCE 27 (1992) 972–982

Aluminium metaphosphate glass-ceramics

M. LANGLET
Laboratoire des Materiaux et du Genie Physique, ENSPG, BP 46, 38402 St Martin D'Heres, France

M. SALTZBERG, R. D. SHANNON
Central Research and Development Department, E. I. Du Pont de Nemours and Co., Experimental Station, Wilmington, DE 19880, USA

AlP_3O_9 glass-ceramics were prepared by crystallization of glasses at 750–1100 °C. Crystallization of AlP_3O_9 and $AlPO_4$ at lower temperatures is favoured by addition of 5–10 mol % Li_2O, Na_2O or AlF_3, whereas crystallization is hindered by 5–10 mol % B_2O_3, BPO_4, SiO_2, TiO_2, Nb_2O_5 or Ta_2O_5. Additives such as TiO_2, ZrO_2, MgF_2, CaF_2 and Pt, frequently useful in nucleating silicate glasses, are ineffective in AlP_3O_9 glasses. $AlPO_4$, resulting from the P_2O_5 loss during melting, forms at the surface of melted glass samples. AlP_3O_9 forms in the bulk as elongated columnar or lamellar crystals with grain sizes of 0.5–2.0 μm. Li_2O-doped AlP_3O_9 is inhomogeneous with coarse intergranular regions and glassy regions. Dielectric constants vary from 5.0–5.2.

1. Introduction and background

The commercial development of glass-ceramics has promoted interest in the study of the mechanism of glass crystallization [1–28]. Most studies have been concerned with aluminosilicate glass-ceramics because of their unique thermal properties, in particular, thermal stability and shock resistance [14, 25]. Recently, alkaline earth phosphate glass-ceramics have been studied [5, 29–41]. By comparison, little is known about M_2O_3–P_2O_5 glass-ceramics (M = Al, Ga, In, Co, Fe, Cr, Mn, V) and their properties. Kishioka and co-workers [7, 42] have determined the regions of glass formation in M_2O–Al_2O_3–P_2O_5 (M = Li, Na, K) and MO–Al_2O_3–P_2O_5 (M = Mg, Ca, and Ba) three-component systems and discussed the glass structure and the effect of the addition of Al^{3+}. Quackenbush and co-workers [43, 44] described the formation and properties of glass in the Al_2O_3–B_2O_3–P_2O_5 system and MacDowell and Wilson [45] discussed the use of Al_2O_3–B_2O_3–P_2O_5 glass-ceramics in high-temperature lighting applications and as a seal for molybdenum or tungsten. Optical properties and chemical stability of glasses in the system $Al(PO_3)_3$–BaF_2–AlF_3 were studied by Galant and co-workers [46, 47]. The ternary system MgO–Al_2O_3–P_2O_5 was investigated by Gonzalez and Halloran [48]. However, the crystallization processes and the crystalline phases in these different glass-ceramic systems have generally not been reported. Zheng *et al.* [8] have studied the crystallization of Al_2O_3–P_2O_5–ZrO_2 glass-ceramics but, up to now, there is little information on aluminophosphate glass-ceramics.

The glass formation and the crystallization process of glass-ceramics in the system Al_2O_3–P_2O_5 close to the AlP_3O_9 composition are described here. The AlP_3O_9 base composition was modified using two kinds of additives. The effect of the compounds Li_2O, B_2O_3, BPO_4 and SiO_2, which are commonly used in glass compositions and which are thought to modify glass melting behaviour, were investigated. AlF_3 was added as well, because this compound was previously reported to reduce the tendency to crystallize [47]. Nucleating agents frequently used for aluminosilicate glass-ceramics were used: TiO_2, ZrO_2, MgF_2, CaF_2, and LaF_3 [10, 12, 14, 22, 25]. The properties of the resulting glass and crystalline phases were investigated using differential thermal analysis (DTA), thermomechanical analysis (TMA), X-ray diffraction (XRD), chemical analysis and scanning electron microscopy.

2. Experimental procedure

2.1. Glass preparation

The starting materials were AlP_3O_9, $LiOH \cdot H_2O$, H_3BO_3, BPO_4, SiO_2, Cr_2O_3, Fe_2O_3, Nb_2O_5, Ta_2O_5, $NaH_2PO_4 \cdot H_2O$, MgP_2O_6, ZnO, KH_2PO_4, ZrO_2, TiO_2, AlF_3, MgF_2, NiF_2, LaF_3 and CaF_2. Typically, 25 g batches were mixed in an automatic mortar for 30 min. In the case of P_2O_5-excess compositions, the batch was precalcined at 500 °C for 150 min in order to minimize P_2O_5 volatilization. Melting was done in an open platinum crucible placed in a furnace previously heated to temperatures ranging from 1450–1500 °C. The samples were held at the melting temperature for 15–30 min and quenched by pouring on to an aluminium plate. Lower melting temperatures were not suitable because of the high viscosity of the melt. In order to minimize P_2O_5 vaporization, the melting time and temperature were < 30 min and < 1500 °C, respectively. Thermal properties of the glasses were investigated by TMA and DTA. Infrared

0022–2461

spectra and chemical analyses were obtained on small glass pieces and the densities of samples before and after crystallization were measured by the flotation method using bromoform and acetone.

2.2. Crystallization

In one scheme (A), ~ 5 g glass pieces were placed on an alumina tray and preheated during a 1 h heating ramp from 500 °C to 700 °C. According to MacDowell and Wilson [45] in aluminosilicate systems, this short preheating treatment provides nucleation sites for the growth of crystals during the subsequent crystallization step. In order to define the crystallization temperature range, samples were then heated individually for 1 h at 800, 900, 1000 and 1100 °C. In this way the complete crystallization process from nucleation to the final crystallization could be followed and the separation of different phases could be correlated with the heat treatment. In a second scheme (B), glass pieces were heated for 24 h at each of a series of temperatures starting at 500 °C. Heating was cumulative so that a sample crystallizing at 700 °C had previously been heated for 24 h at 500, 550, 600 and 650 °C. Crystallization temperatures higher than 1100 °C were not studied because of the AlP_3O_9–$AlPO_4$ eutectic at about 1200 °C. Development of opacity was assumed to be an indication of crystal formation. Samples were then finely ground and phase identification was made by X-ray diffraction.

Scanning electron microscope studies were undertaken on both polished and fracture surface. Chemical compositions of observed areas were investigated using X-ray fluorescence analysis. Etching of polished surfaces with 0.5% NaOH solution was performed to obtain information on the nature of the multiphase structures. Both AlF_3- and Li_2O-doped samples were studied as a function of crystallization temperature.

High-temperature XRD data were obtained on a Rigaku θ–θ diffractometer equipped with a 1600 °C hot-stage. Crystallization experiments were run in two modes. In the first, the temperature was slowly increased, typically at 1–5 °C min^{-1}, and X-ray patterns were taken at regular intervals. This type of experiment allowed the crystallization temperatures of the glass to be determined. In the second mode, isothermal experiments at or near the crystallization temperature were also carried out to determine qualitatively the kinetics of the crystallization process and the order of phase appearance.

3. Results

3.1. Glass melting

Batch compositions are reported in Table I. All the compositions yielded transparent glasses. The purple colour of TiO_2-doped glass was assumed to indicate the presence of Ti^{3+}. The high acidity of phosphate glasses apparently leads to reduction of Ti^{4+} and other easily reduced ions, such as Mo^{6+} and W^{6+}. Melts containing Li_2O and SiO_2 were very fluid and led to a good glass transparency. In the other cases, the melt viscosity was higher. These glasses also exhibited a slight opacity on their surface, which is related to the formation of $AlPO_4$ on the glass surface during the early stages of cooling. This type of crystallization was not observed for Li_2O- and SiO_2-doped glasses.

As indicated in previous studies of AlP_3O_9 glass formation [7, 43], considerable loss of P_2O_5 occurred during melting. As shown in Table I, melting of the AlP_3O_9 compositions led to a P/Al ratio of about 2.30, well below the stoichiometric value. The use of additives to the AlP_3O_9 composition led to variations of the P/Al ratio ranging from about 2.60–2.20 and corresponding to P_2O_5 loss of about 15%–25%. Lowering the melting temperature from 1500–1450 °C in the case of the 10% Li_2O composition did not lead to an increase of the P_2O_5 content in the glass. Using a P_2O_5 excess in the batch compositions of two-component systems had a limited effect on the loss of P_2O_5, but excess P_2O_5 in the presence of Li_2O increased the P/Al ratio to 2.7–2.9 (see Table I).

Although AlF_3, MgF_2, CaF_2 and LaF_3 were used as additives, no fluorine remained after melting. According to Galant and Urusovskaya [46] and Ehrt *et al.* [49], fluorine is lost as the volatile product POF_3 at temperatures as low as 600 °C.

3.2. Glass-ceramic formation

Glass devitrification temperatures using the two crystallization schemes are given in Table I. Devitrification was assumed to be complete when no significant glassy area could be observed on the sample surface and interior. Further confirmation of crystallization was obtained from strong XRD peaks of AlP_3O_9 and $AlPO_4$. For most samples, opaque areas were observed on the glass surface at least 100 °C below the temperatures given in Table I. The crystallization begins at the surface of the samples and progresses to the centre, and full crystallization can be obtained at temperatures lower than those we list as the devitrification point given sufficient time.

The lowest devitrification temperatures were observed for Li_2O- and AlF_3-doped glasses (T_c = 800 and 900–1000 °C, respectively, for glasses crystallized according to scheme A). $NaPO_3$ was also effective in reducing devitrification temperatures. Devitrification was enhanced as the Li_2O content was increased from 5%–10%. This was not the case when the AlF_3 content was increased from 5%–10%. Most of the other glasses crystallized between 1000 and 1100 °C. Above 1000 °C, crystallization was accompanied by void formation inside the samples. B_2O_3- and SiO_2-doped glasses did not lead to well-crystallized glass-ceramics. Crystallization of the 5% B_2O_3-doped glass began at 1000 °C but was followed by partial melting at 1100 °C as indicated by a significant increase of the XRD background. The 10% B_2O_3- and 5% and 10% BPO_4- and SiO_2-doped glasses crystallized only at the surface at 1100 °C. Glassy or opalescent areas remained in the core of the sample. TiO_2-doped glasses remained largely in a glassy state showing that this dopant inhibits crystallization.

Nucleating agents usually effective in silicate glass-ceramics were not effective in AlP_3O_9 glasses. None of

TABLE I Glass compositions and crystallization data

Batch composition (mol %)	$\frac{P}{Al}$ in glass	Devitrification temperature (°C) and appearance		Crystal phases after devitrification[c]
		1[a]	2[b]	
AlP_3O_9[d]	2.30	850	1000–1100 white	AlP_3O_9, $AlPO_4$
$85AlP_3O_9 \cdot 15P_2O_5$	2.40		1000–1100 white	AlP_3O_9, $AlPO_4$
$70AlP_3O_9 \cdot 30P_2O_5$	2.34		1000–1100 white	AlP_3O_9, $AlPO_4$
$95AlP_3O_9 \cdot 5Li_2O$	2.31	500	800 white	AlP_3O_9, $AlPO_4$
$90AlP_3O_9 \cdot 10Li_2O$	2.60		700–800 white	AlP_3O_9, $AlPO_4$
$95AlP_3O_9 \cdot 5B_2O_3$	2.36	900	1000 white	AlP_3O_9, $AlPO_4$; crystal to amorphous ratio strongly decreased at 1100 °C
$90AlP_3O_9 \cdot 10B_2O_3$	–		1100 partially glassy opalescent	–
$95AlP_3O_9 \cdot 5BPO_4$	2.40	900	1100 partially glassy opalescent	AlP_3O_9, $AlPO_4$
$90AlP_3O_9 \cdot 10BPO_4$	–		1100 partially glassy opalescent	–
$95AlP_3O_9 \cdot 5SiO_2$	2.50	850–900	1100 partially glassy opalescent	AlP_3O_9, $AlPO_4$
$90AlP_3O_9 \cdot 10SiO_2$	–		1100 partially glassy	–
$95AlP_3O_9 \cdot 5AlF_3$	2.30	750	900–1000 white	AlP_3O_9, $AlPO_4$
$90AlP_3O_9 \cdot 10AlF_3$	2.21		1000 white	AlP_3O_9, $AlPO_4$
$95AlP_3O_9 \cdot 5LaF_3$	2.57	850–900	1100 opalescent	AlP_3O_9, $AlPO_4$
$95AlP_3O_9 \cdot 5MgF_2$	2.42	850	1000–1100 white	AlP_3O_9, $AlPO_4$
$95AlP_3O_9 \cdot 5CaF_2$	2.54	800–850	1000 white	AlP_3O_9, $AlPO_4$
$95AlP_3O_9 \cdot 5ZrO_2$	2.47	900	1000–1100 white	AlP_3O_9, $AlPO_4$; $AlPO_4$ does not appear at 1100 °C
$95AlP_3O_9 \cdot 5TiO_2$	2.53		no devitrification; purple	–
$99.95AlP_3O_9 \cdot 0.05$ Pt	–	850–900		AlP_3O_9, $AlPO_4$
$97.5AlP_3O_9 \cdot 2.5Cr_2O_3$	–	850–900		AlP_3O_9, $AlPO_4$
$97.5AlP_3O_9 \cdot 2.5Fe_2O_3$	–	800–850		AlP_3O_9, $AlPO_4$
$95AlP_3O_9 \cdot 5NaPO_3$	–	700–750		AlP_3O_9, $AlPO_4$
$95AlP_3O_9 \cdot 5KPO_3$	–	800–850		
$95AlP_3O_9 \cdot 5MgP_2O_6$	–	850–900		
$95AlP_3O_9 \cdot 5ZnP_2O_6$	–	800–850		
$95AlP_3O_9 \cdot 5NiP_2O_6$	–	850–900		AlP_3O_9, $AlPO_4$
$95AlP_3O_9 \cdot 2.5Nb_2O_5$	–	900		
$95AlP_3O_9 \cdot 2.5Ta_2O_5$	–	> 900		

[a] Crystallization schedule: 500 °C (24 h); 550 °C (24 h); 600 °C (24 h); etc. until devitrification occurs.
[b] Crystallization schedule: 500 → 700 °C in 1 h followed by 1 h at 800, 900, 1000 or 1100 °C.
[c] For all the compositions reported in this table, $AlPO_4$ concentration was consistently lower than AlP_3O_9 concentration.
[d] Batch slowly heated from room temperature to 1500 °C over a 17 h period and kept at 1500 °C for 15 min.

the compounds TiO_2, ZrO_2, MgF_2, CaF_2 or LaF_3 led to a significant lowering of the glass devitrification temperature. Small amounts of platinum (0.01%–0.02% in weight) were present both in the glass and in the initial AlP_3O_9 reagent. The impurity did not enhance the crystallization of the glass as confirmed by the addition of 0.05% Pt to the melt (see Table I).

3.3. Thermal analysis

Thermal analysis (TMA, DTA) provided some information on the glass crystallization behaviour. TMA and DTA results are summarized in Tables II and III. TMA was conducted in the range 20–1150 °C and DTA in the range 20 to ~ 1400 °C.

TMA allowed the determination of the thermal

TABLE II TMA results

Composition	T_g (°C)	T_d (°C)
AlP_3O_9	790	840
$95AlP_3O_9 \cdot 5Li_2O$	700	740
$90AlP_3O_9 \cdot 10Li_2O$	640	690
$95AlP_3O_9 \cdot 5AlF_3$	780	830
$95AlP_3O_9 \cdot 5MgF_2$	770	820
$95AlP_3O_9 \cdot 5CaF_2$	765	810
$95AlP_3O_9 \cdot 5ZrP_4O_{12}$	768	823
$95AlP_3O_9 \cdot 5TiO_2$	789	–
$AlP_3O_9 \cdot 5SiO_2$	781	812
$AlP_3O_9 \cdot 5B_2O_3$	764	806

TABLE III DTA results

Batch composition	Crystallization peaks (°C)	Melting peak (°C)
AlP_3O_9	916[a], 1110	1210
$70AlP_3O_9 \cdot 30P_2O_5$	1065	1210
$95AlP_3O_9 \cdot 5LaF_3$	900[a], 1130	–
$95AlP_3O_9 \cdot 5MgF_2$	900[a], 1080	–
$95AlP_3O_9 \cdot 5CaF_2$	1080	1210
$95AlP_3O_9 \cdot 5ZrO_2$	940[a], 1120	1210
$95AlP_3O_9 \cdot 5Li_2O$	880	1240
$90AlP_3O_9 \cdot 10Li_2O$	700	1240
$95AlP_3O_9 \cdot 5B_2O_3$	1060[a]	1160
$90AlP_3O_9 \cdot 10B_2O_3$	Not discernible	Not discernible
$95AlP_3O_9 \cdot 5BPO_4$	1100	1180
$90AlP_3O_9 \cdot 10BPO_4$	Not discernible	Not discernible
$95AlP_3O_9 \cdot 5SiO_2$	940[a], 1080	Not discernible
$90AlP_3O_9 \cdot 10SiO_2$	1100	Not discernible
$95AlP_3O_9 \cdot 5AlF_3$	1020	1215
$90AlP_3O_9 \cdot 10AlF_3$	915[a], 1020	1215

[a] Weak and broad peak.

expansion coefficient, the glass transition temperature, T_g, and the deformation temperature, T_d, of the glass [50, 51]. The nucleation treatments used were in a temperature range from about 200 °C below T_g to 50 °C above T_g. For all the compositions, the thermal expansion coefficient ranged from 4.5–6.5 p.p.m. $°C^{-1}$ for temperatures ranging from 20–600 °C.

In the case of the 5% Li_2O-doped sample, TMA was performed before and after annealing at 700 °C. Before annealing, the sample contracted ~ 1% above T_d as softening occurred (see Fig. 1). After annealing, similar values of T_g and T_d were obtained but above T_d, crystallization of AlP_3O_9 resulted in continuous expansion. Thus, annealing at 700 °C provides an effective method of nucleating AlP_3O_9 in Li_2O-doped samples.

A typical DTA curve (Fig. 2) obtained during crystallization mainly shows one or more exothermic peaks related to the appearance of crystalline phases and one or more endothermic peaks due to the melting of these crystal phases. When devitrification was observed to occur above 1000 °C, in some cases, DTA curves showed a weak and broad exothermic peak located at about 900 °C. The origin of this broad exotherm, which occurred in only a few compositions, is not known. The observed devitrification temperatures (from the 1 h annealing experiments) were in rather good agreement with the largest DTA crystallization peak. In the case of Li_2O- and AlF_3-doped glasses, rather sharp crystallization peaks indicated evidence of a fast process. Very weak and broad peaks, or the absence of peaks in the case of B_2O_3- or BPO_4-doped glasses, clearly showed a relatively slow crystallization behaviour.

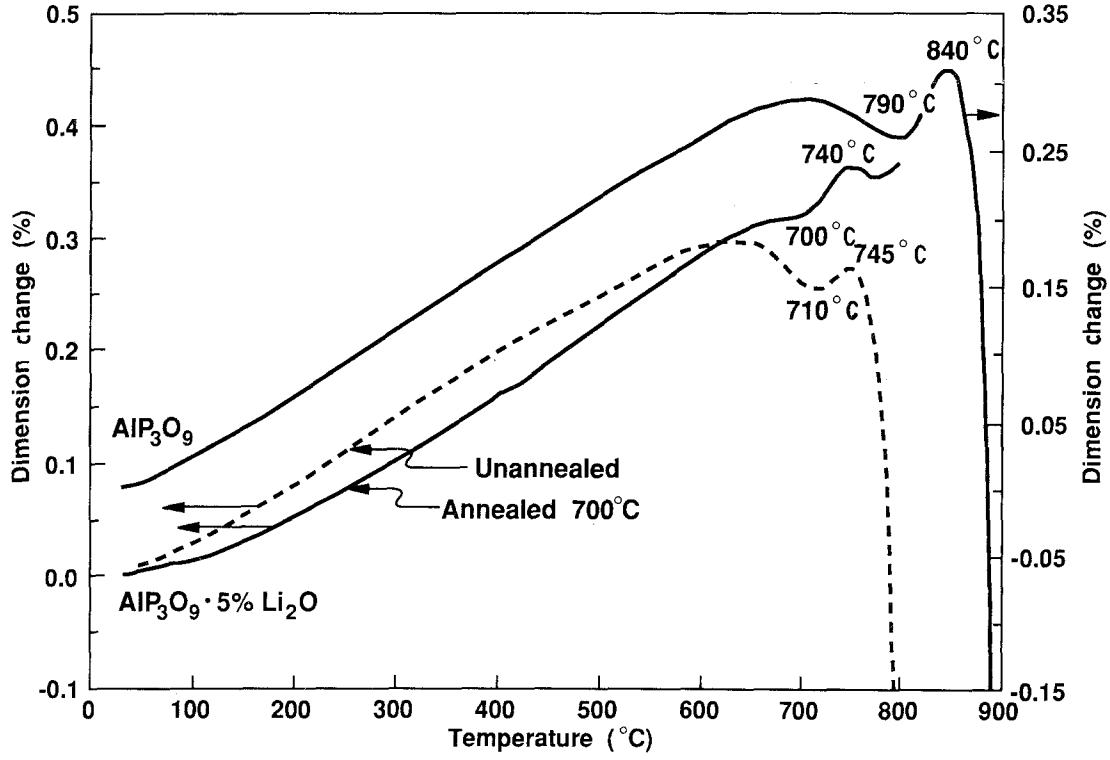

Figure 1 TMA curves for: (a) pure AlP_3O_9 glass, (b) AlP_3O_9–5% Li_2O glass, (c) AlP_3O_9–5% Li_2O glass preheated at 700 °C.

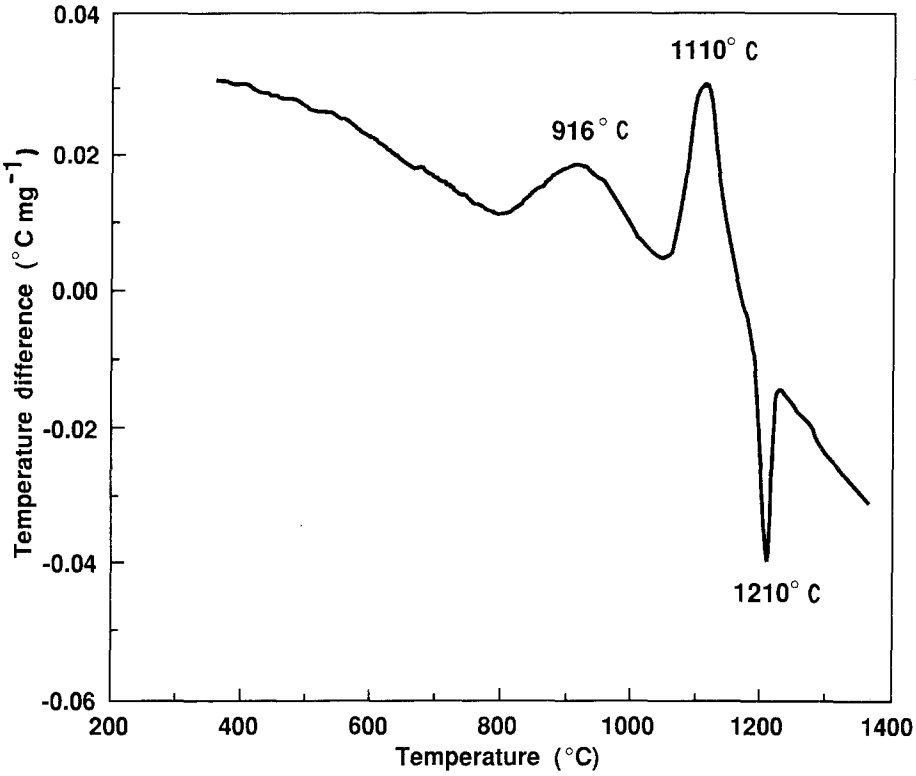

Figure 2 DTA curve for AlP_3O_9 glass.

The DTA results confirmed the lack of effectiveness of common nucleating agents in catalysing the aluminophosphate glass crystallization. These results are to be compared with those of Kishioka *et al.* [7] who crystallized glasses in the system Li_2O–Al_2O_3–P_2O_5 at temperatures as low as 800 °C and those of Zheng *et al.* [8] who did not succeed in crystallizing glasses in the system ZrO_2–Al_2O_3–P_2O_5 below 1150 °C.

3.4. X-ray powder diffraction

3.4.1. Crystallized samples

All devitrified glass X-ray patterns exhibited sharp lines of cubic aluminium metaphosphate, AlP_3O_9 ($a = 1.3729$ nm). This phase was previously reported [52] as the only form stable at high temperature among the five known AlP_3O_9 species. No other AlP_3O_9 phases were identified by XRD.

All devitrified glass-ceramics contained $AlPO_4$ owing to the P_2O_5 deficit in the sample. There was always less $AlPO_4$ than AlP_3O_9 and the ratio of $AlPO_4/AlP_3O_9$ was not significantly affected by the presence of additives.

Two forms of $AlPO_4$ were identified. The high-cristobalite form of $AlPO_4$ (high-C-$AlPO_4$; [53, 54]) was identified in the Li_2O- and AlF_3-doped samples after crystallization at 800 or 900 °C. After crystallization at 1000 or 1100 °C, new weak lines at $d = 0.408$, 0.316, 0.286, and 0.250 nm appear, indicating presence of the low-cristobalite form of $AlPO_4$ (low-C-$AlPO_4$; [56–58]). X-ray patterns of many of our samples clearly showed the presence of both low- and high-cristobalite forms. Increasing crystallization temperature from 800 to 1100 °C caused a decrease in the amount of high-C-$AlPO_4$ and an increase in the amount of low-C-$AlPO_4$ present at room temperature.

As indicated in Table I, in several compositions containing a variety of nucleating agents, the concentration of $AlPO_4$ decreased as the crystallization temperature increased. When crystallization occurred at 1100 °C, $AlPO_4$ did not appear at all and the X-ray pattern exhibited only lines of AlP_3O_9. For Li_2O- or B_2O_3-containing compositions doped with LaF_3, the disappearance of $AlPO_4$ was accompanied by a strong increase of the X-ray background. In all cases, white opaque ceramics were obtained when $AlPO_4$ was present and opalescent ceramics were obtained when $AlPO_4$ was absent after crystallization at 1100 °C. These observations suggested that after heating at 1100 °C, $AlPO_4$ might disproportionate to AlP_3O_9 and Al_2O_3. This hypothesis is not in agreement with Beck [59], who states that the melting point of $AlPO_4$ is > 1600 °C, or Hummel [60] and Shafer and Roy [61], who claim it to be > 1800 °C. However, Horn and Hummel [62] found samples of $95AlPO_4 \cdot 5BPO_4$ heated below 1200 °C and $90AlPO_4 \cdot 5BPO_4 \cdot 5SiO_2$ heated to 1415 °C to contain mixtures of C-$AlPO_4$ and AlP_3O_9.

3.4.2. High-temperature XRD

Complementary high-temperature XRD was performed on representative samples of finely ground glass. Scans were made at every 30 °C while heating the sample at 1 °C min^{-1} from 500 to 1200 °C. High-temperature patterns were somewhat different from the room-temperature patterns. During high-temperature X-ray experiments, $AlPO_4$ disappearance was not observed for compositions doped with nucleating

agents. On the contrary, all the samples exhibited a progressive increase of the $AlPO_4$ content as the temperature increased, probably because of P_2O_5 loss during the experiment. High-temperature X-ray patterns generally confirmed devitrification and DTA experiments showing the appearance of both AlP_3O_9 and $AlPO_4$ at about 680–700 °C for the 5% Li_2O-doped compositions, 890–920 °C for the 5% AlF_3-doped composition and 950–1000 °C for the pure AlP_3O_9 composition.

Only high-C-$AlPO_4$ was present during the high-temperature X-ray experiments. After cooling to room temperature, low-C-$AlPO_4$ appeared. The presence of low-C-$AlPO_4$ observed at room temperature after crystallization above 900 °C is caused by the high to low cristobalite transformation occurring during cooling after the crystallization treatment.

Isothermal high-temperature XRD was undertaken on 5% AlF_3-doped glass in order to study the earlier stages of crystallization. The sample was heated from room temperature to 900 °C in 15 min and isothermal scans were then collected every 7 min between $2\theta = 19°$ and 25°. In this way, the appearance of the main diffraction peaks of AlP_3O_9 ($d = 0.434$ nm) and high-C-$AlPO_4$ ($d = 0.416$ nm) could be related to the heat treatment time at 900 °C. In the case of finely ground glass, AlP_3O_9 crystallization occurred after about 40 min and $AlPO_4$ crystallization about 15 min later. The intensity of both the AlP_3O_9 and $AlPO_4$ diffraction peaks increased progressively during heat treatment. In a second experiment, the surface of a transparent bulk sample showing no opacity was examined. The room-temperature X-ray pattern showed only weak low-C-$AlPO_4$. This suggests that $AlPO_4$ crystallites are already present at the glass surface after cooling the glass, even when no opacity is observed. During heating from room temperature to 900 °C, low-C-$AlPO_4$ transformed to high-C-$AlPO_4$. AlP_3O_9 crystallized after about 100 min heat treatment at 900 °C. Both $AlPO_4$ and AlP_3O_9 increased slowly at 900 °C. A piece taken from the inside of the glass sample was preheated during a 1 h temperature ramp between 500 and 750 °C and then kept at 750 °C for 1 h. This heat treatment was thought to be suitable to initiate nucleation. However, the absence of diffraction peaks indicated that the inside of the glass was free of measurably large crystallites. A weak $AlPO_4$ peak appeared after about 30 min at 900 °C and AlP_3O_9 appeared less than 10 min later. Increase of both $AlPO_4$ and AlP_3O_9 was very slow for 2 h. A sudden increase of the two phases was observed after 120 min heat treatment at 900 °C. This experiment suggests a two-stage crystallization process, consisting of nucleation, followed by a more rapid crystallization process progressing through the bulk of the glass.

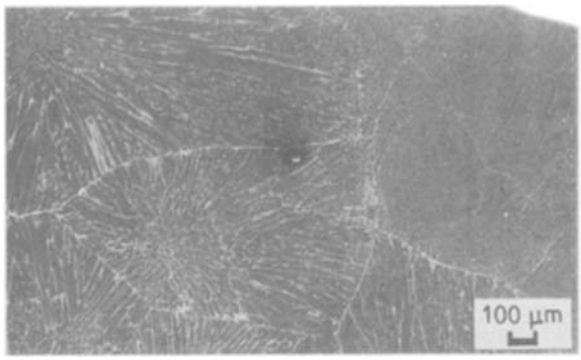

Figure 3 Scanning electron micrograph of polished surface AlP_3O_9–5% Li_2O crystallized at 900 °C, 1 h.

3.5. Electron microscopy studies

Non-devitrified glasses exhibited a homogeneous smooth appearance with no recognizable morphological features. Crystallized samples of Li_2O-doped AlP_3O_9 (Figs 3–5), AlP_3O_9 (Fig. 6) and AlF_3-doped AlP_3O_9 (Figs 7–9) showed different morphologies.

3.5.1. AlP_3O_9

Samples of AlP_3O_9 crystallized at 1100 °C showed surfaces with conchoidal fracture and, in the case of polished samples, smooth surfaces with only a few visible boundaries. A characteristic feature was the presence of ~ 1 µm thick lamellae or columns. Backscatter photographs of polished samples (Fig. 6) showed dark regions between the lamellae or columns which were partially removed upon etching with NaOH (Fig. 6b). As indicated in the next section, these lamellae are AlP_3O_9 and the intergranular region consists of $AlPO_4$. Regions of parallel lamellae oriented in a single direction and extending for 100–500 µm seem to join smoothly with regions of differently oriented lamellae.

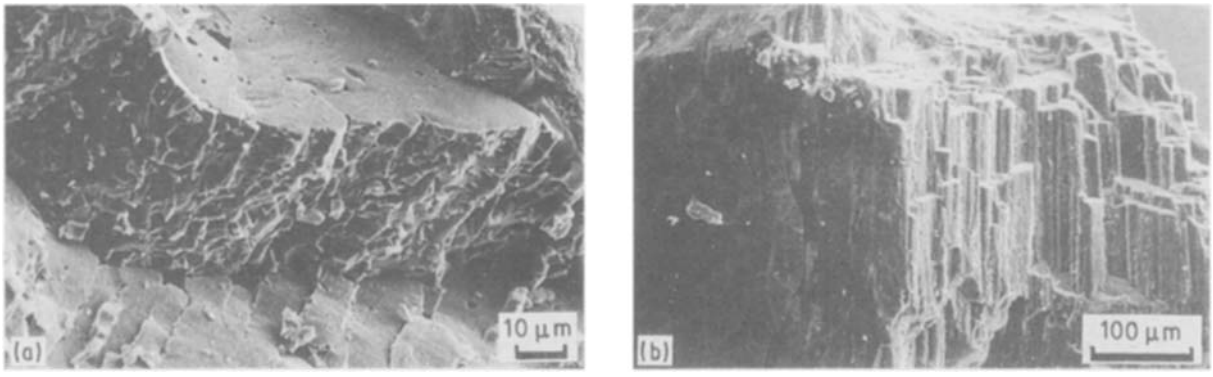

Figure 4 Scanning electron micrographs of fracture surfaces of AlP_3O_9–5% Li_2O crystallized at 900 °C, 1 h.

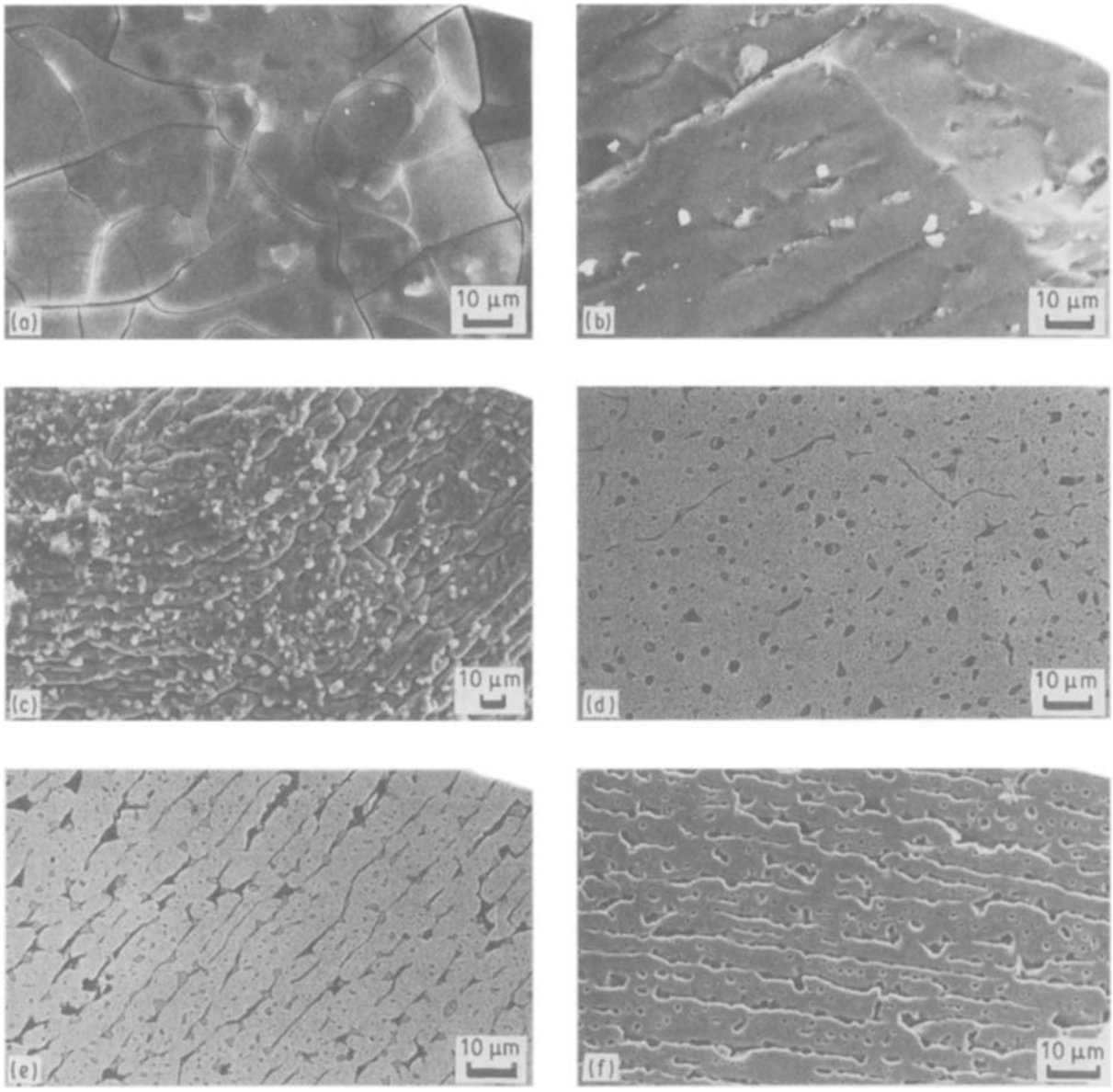

Figure 5 Scanning electron micrographs of AlP_3O_9–5% Li_2O (a) crystallized at 900 °C, 1 h, (b) crystallized at 1100 °C, 1 h, fracture surface, (c) crystallized at 1000 °C, 1 h, fracture surface, (d) crystallized at 800 °C, 1 h, polished surface backscatter photograph, (e) crystallized at 1000 °C, 1 h, backscatter photograph, (f) crystallized at 1000 °C, 1 h, etched in 5% NaOH for 10 min.

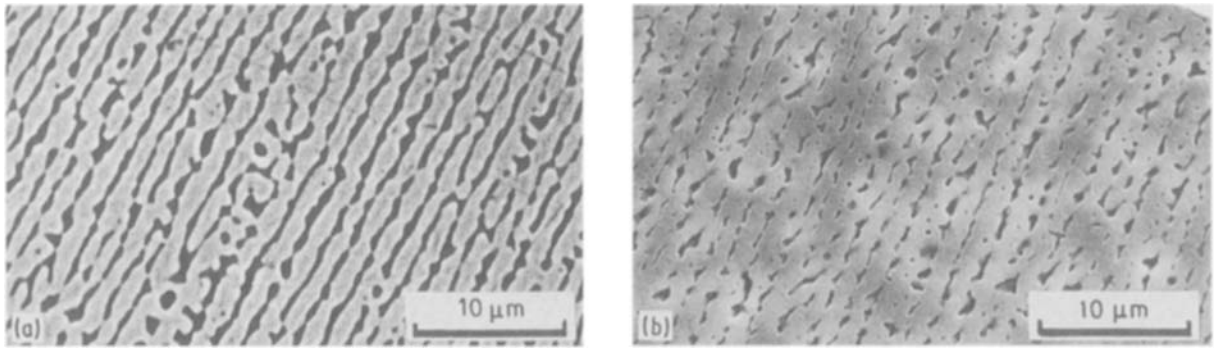

Figure 6 SEM backscatter micrographs of AlP_3O_9 (a) crystallized at 1100 °C, 1 h, polished surface, (b) crystallized at 1100 °C, 1 h, polished surface, etched 10 min in 5% NaOH.

3.5.2. $95AlP_3O_9 \cdot 5AlF_3$

AlF_3-doped samples were observed after crystallization at 900, 1000 and 1100 °C. Clean fractures were obtained with the AlF_3-doped composition. No voids were visible after fracture. The fractured and polished surfaces of the sample crystallized at 900 °C had a smooth appearance (Fig. 7a and b) suggesting the presence of crystallites of AlP_3O_9 and $AlPO_4$ too

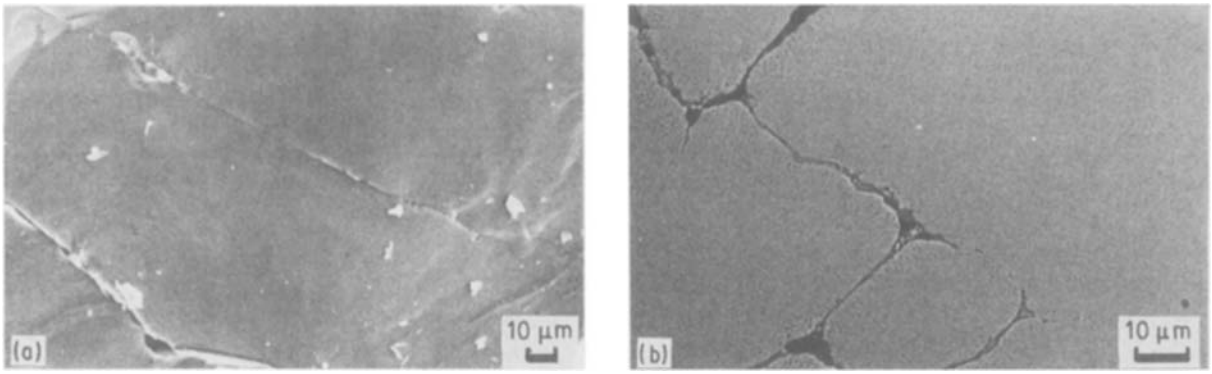

Figure 7 Scanning electron micrographs of AlP_3O_9–5% AlF_3 crystallized at 900 °C, 1 h: (a) fracture surface, (b) polished surface.

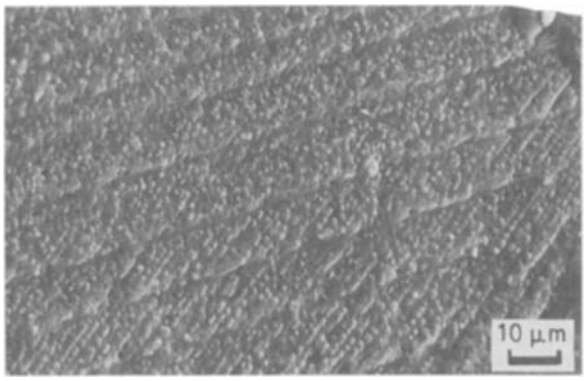

Figure 8 Scanning electron micrograph of fracture surface of AlP_3O_9–5% AlF_3 crystallized at 1100 °C, 1 h.

small to be resolved by the SEM. Etching with 0.5% NaOH for 10 min resulted in no change in surface structure. The cracks evident in Fig. 7 are possibly caused by thermal stress effects. An average P/Al ratio of 2.7 measured on large areas at low magnification confirmed the glass-ceramic P_2O_5 deficit found by chemical analysis (P/Al = 2.30).

Polished samples of AlF_3-doped AlP_3O_9 crystallized at $T > 1000$ °C were characterized by 100–500 μm grains composed of smaller elongated crystallites. Within these grains, fracture surfaces of samples crystallized at 1000 and 1100 °C (Fig. 8) showed no cracks and exhibited regular alignments of 0.5–2.0 μm thick crystallites distributed in a lamellar matrix similar to those in Fig. 6a. A P/Al ratio of about 1 ($AlPO_4$) was measured for the grains while the P/Al ratio for the matrix was close to 3 (AlP_3O_9). Polished surfaces for the AlF_3-doped samples were observed with SEM using backscattered electrons (Figs 7b, 9a and b). The smooth uniform aspect of samples crystallized at 900 °C was confirmed (Fig. 7b) while regular alignments of small dark spots were observed in the case of samples crystallized at 1000 or 1100 °C (Fig. 9a). Backscatter electron photographs are sensitive both to surface topography and composition effects and lead to darker areas in regions containing both voids and lighter elements. Therefore, the observed dark areas are related to the $AlPO_4$ grains and/or alignments of voids observed on fractured surfaces. Etching a polished section with NaOH removed the grains and left the lamellar or columnar matrix (Fig. 9b). Analysis of the remaining lamellar area showed it to be AlP_3O_9 and confirmed that the micrometre-sized grains were $AlPO_4$. There were no clearly observable grain boundaries in the AlP_3O_9 matrix showing that even after crystallization at higher temperature the $AlPO_4$ grains must be homogeneously distributed in a glassy or crystalline AlP_3O_9 matrix.

3.5.3. $95AlP_3O_9 \cdot 5Li_2O$

Li_2O-doped samples with or without nucleating agents had a different appearance from pure AlP_3O_9 or AlF_3-doped samples. Fracture surfaces exhibited inhomogeneous morphology consisting of smooth

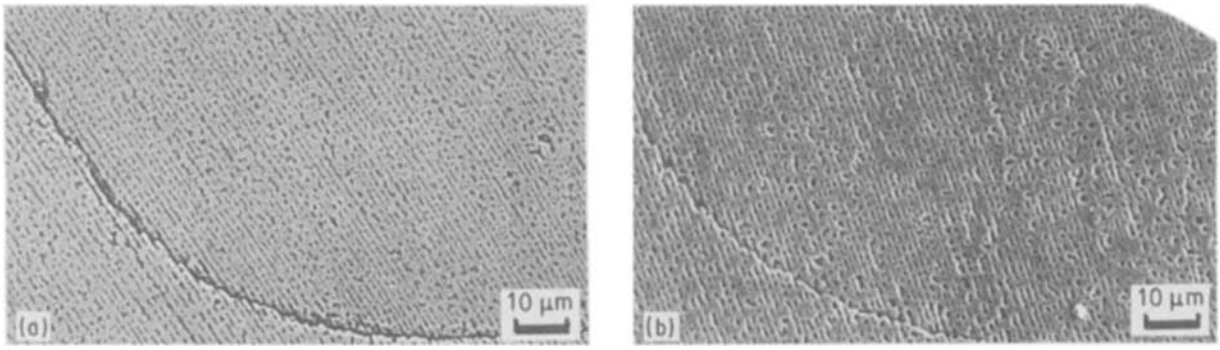

Figure 9 Scanning electron micrographs of polished surfaces of AlP_3O_9–5% AlF_3 crystallized at 1000 °C, 1 h: (a) backscatter, (b) etched with 5% NaOH for 10 min.

surfaces, coarse granular regions and cracked glassy areas either smooth or containing micrometre-sized grains.

One feature noted in fracture surfaces of Li_2O-doped AlP_3O_9 crystallized at 900 °C is the presence of both columns and lamellae (Fig. 4a and b). The presence of columnar grains or fibrils was previously noted by Abe *et al.* [32, 36, 40, 41] in CaP_2O_6. Samples crystallized at 800 and 900 °C showed many regions with a smooth glassy appearance containing many internal cracks (Fig. 5a). These regions sometimes contained inhomogeneously distributed $AlPO_4$ grains. The large glassy areas showed a P/Al ratio ranging from 5–8 which suggested that the matrix consisted of $LiPO_3$ glass or a lithium aluminium phosphate glass. The formation of the glassy phase is consistent with the observed $T_d = 740$ °C.

After crystallization at 1000 or 1100 °C, many inhomogeneously distributed smooth areas were observed (Fig. 5b), whereas they were not observed for the other compositions. Other areas showed a lamellar structure with many associated $AlPO_4$ crystallites (Fig. 5c). Crystallization at 1000 or 1100 °C led to an increase in the number of $AlPO_4$ grains. The grains were larger (2–10 μm) and the grain distribution more inhomogeneous than for the other compositions examined.

Polished samples of Li_2O-doped AlP_3O_9 crystallized at $T > 800$ °C and AlF_3-doped AlP_3O_9 crystallized at $T > 1000$ °C were characterized by 100–500 μm grains composed of smaller elongated crystallites (see Fig. 3). The formation of these large grains seems to coincide with the DTA crystallization peaks. The regions within the grains show a diversity of character. Backscatter electron studies on polished surfaces also indicated cracks, inhomogeneously distributed glassy areas and $AlPO_4$ grains (Fig. 5d and e). Etching for 10 min with NaOH dissolved large amounts of intergranular material ($AlPO_4$?) and smaller spherical volumes inside the lamellae ($LiPO_3$?) as shown in Fig. 5f.

A consistent feature of the Li_2O-doped AlP_3O_9 is the dramatic increase in the size of both $AlPO_4$ crystallites and the AlP_3O_9 lamellae or fibrils. Whereas in undoped and AlF_3-doped AlP_3O_9, crystallite and fibril size remained below 1–2 μm, sizes of 2–10 μm were commonly observed in the Li_2O-doped samples. This is consistent with the lower viscosity of the Li_2O-doped glasses.

3.6. Density and dielectric measurements

All the glasses exhibited densities of about 2.60 g cm^{-3}, in good agreement with values previously reported [8, 42] for glass compositions close to AlP_3O_9. All the compositions crystallized at 900 or 1000 °C exhibited densities ranging from 2.40–2.60 g cm^{-3}. These values are consistent with the ceramic compositions which are assumed to be composed of a crystallized AlP_3O_9 matrix ($d = 2.709$ g cm^{-3}), $AlPO_4$ embedded in the matrix ($d = 2.164$ g cm^{-3} for high-C-$AlPO_4$ and $d = 2.304$ g cm^{-3} for low-C-$AlPO_4$) and perhaps some remnant glass ($d = 2.60$ g cm^{-3}). Crystallization was observed to proceed from the outside surface to the inner core of the glass-ceramic. Without a compensating sample shrinkage, complete crystallization of the glassy core to the more dense AlP_3O_9 led to the appearance of voids in samples crystallized at $T > 1000$ °C. A slower crystallization process with more remnant glass was thought to favour a better glass-ceramic density. This was confirmed by the lack of voids in samples crystallized below 1000 °C.

Dielectric properties were measured in the range 10 kHz–1 MHz on glass samples 10 mm × 10 mm × 1 mm in size. Dielectric constant and dielectric loss showed a weak dependence on frequency. All the glass compositions showed similar dielectric properties with dielectric constants ranging from 5.04–5.17 consistent with the AlP_3O_9 single crystal value of 5.18. Dielectric losses (tan δ) of the glasses, in the range 0.001–0.003, are considerably higher than those found for the crystal of 0.0006.

4. Discussion

Loss of P_2O_5 during melting leads to glass compositions intermediate to AlP_3O_9 and $AlPO_4$ and to the appearance of $AlPO_4$ crystallites in the AlP_3O_9 melt. The formation of the slightly opaque thin film, occasionally observed on the surface of glasses during cooling, showed that the formation of $AlPO_4$ crystallites on the glass surface occurred in the case of viscous melts and did not occur in the case of fluid melts.

The high cristobalite form of $AlPO_4$ (high-C-$AlPO_4$) is stabilized in the crystallized AlP_3O_9 glass-ceramics studied here. It is known [59] that high-C-$AlPO_4$, in the absence of a glassy matrix, generally reverts to low-C-$AlPO_4$ at about 210 °C. Chemical stabilization of high-C-$AlPO_4$ at room temperature has been previously obtained only in the case of solid solution with BPO_4 cristobalite in sealed systems [62]. In our case, primarily high-C-$AlPO_4$ was observed at 800 or 900 °C in Li_2O- and AlF_3-doped glass-ceramics. In these cases, solid solution formation is not likely as a mechanism for stabilization of high-C-$AlPO_4$ to room temperature. We therefore suggest that high-C-$AlPO_4$ nuclei could be formed during melting of AlP_3O_9 glass at 1500 °C and could be mechanically stabilized by a surrounding glass matrix which prevented the high–low $AlPO_4$ phase transition during cooling. Such a possibility was also considered by Horn and Hummel [62] when trying to explain high-C-$AlPO_4$ stabilization by BPO_4 additions. The appearance of low-C-$AlPO_4$ when cooling from a crystallization temperature above 900 °C could be related to a decrease of the glass viscosity or the amount of glass in the AlP_3O_9 glass-ceramic.

On the basis of XRD and DTA results, SiO_2, B_2O_3 and BPO_4 additions stabilize AlP_3O_9 glass and inhibit crystallization, whereas Li_2O, Na_2O, and to a lesser extent, AlF_3, enhance aluminophosphate glass crystallization leading to mixed $AlPO_4$–AlP_3O_9 glass-ceramics. In all cases, crystallization is strongly surface-nucleated. It is believed that metaphosphate glasses are composed of polyphosphate anion chains cross-linked by metal–oxygen bonds. Weakening these cross-linking bonds (e.g. substitution of Al^{3+} by

Li^+) lowers the viscosity and the crystallization temperature of the glasses. When SiO_2 or B_2O_3 are present in the structure, they can be expected to form strong bonds between chains, and thus, stabilize the glassy phase. Our results indicated that the SiO_2- and B_2O_3-containing glasses crystallize to AlP_3O_9 and/or $AlPO_4$; thus, as crystallization proceeds, the glass-forming additive is concentrated in the residual glass. Once the concentration of the glass-former in the residual glass reaches some critical level, crystallization ceases, as indicated by the presence of significant quantities of remnant glass in these samples even after heat treatment at 1100 °C for 24 h.

Another important factor in the crystallization of aluminium metaphosphate glasses is the phosphate chain length which is controlled by the P_2O_5/modifier ratio. It appears that when the P/Al ratio in the glasses decreases (shortening the average chain length), the crystallization temperature also decreases. Smaller P/Al ratios promote the formation of $AlPO_4$ which, based on our XRD results, is present on the surfaces of the as-made glasses. Because we have seen that the crystallization is strongly surface nucleated, we conclude that these $AlPO_4$ nuclei, heterogenously formed during the glass melting, are sites where the subsequent crystallization of $AlPO_4$ and AlP_3O_9 occurs. This scenario is consistent with the microstructures we have observed by SEM, where small $AlPO_4$ grains are distributed in a lamellar or columnar matrix of AlP_3O_9.

It appears that the effects of the heterogenously formed $AlPO_4$ nuclei overshadow the effects of the additives we have investigated as potential crystallization aids. The only additives which had a measurable effect on the crystallization behaviour were those which lowered the viscosity (Li_2O or Na_2O), decreased the P/Al ratio (AlF_3), or were glass formers which concentrated in the residual glass during crystallization (SiO_2 and B_2O_3). The other additives, which have proven so effective in promoting crystallization in silicate glass-ceramics, had little measurable effect.

5. Conclusions

A series of AlP_3O_9 glasses, modified with a variety of metal oxides and fluorides, was melted at 1450 °C. These glasses crystallized to AlP_3O_9 and $AlPO_4$ at temperatures of 750–1100 °C. The $AlPO_4$, found at the surface of the melted glass samples, results from P_2O_5 loss during melting. Crystallization at 800–900 °C favours the high-cristobalite form of $AlPO_4$, whereas crystallization at 1000–1100 °C favours the low-temperature form. Additives used were: B_2O_3, SiO_2, BPO_4, MgF_2, CaF_2, LaF_3, TiO_2, ZrO_2, Cr_2O_3, Fe_2O_3, Nb_2O_5, Ta_2O_5, $NaPO_3$, KPO_3, MgP_2O_6, ZnP_2O_6, and NiP_2O_6. The most effective crystallization promoters are Li_2O, $NaPO_3$, and AlF_3 which allow crystallization at 500, 700, and 750 °C, respectively, in 24 h. Most glasses crystallized at 850–900 °C. The additives B_2O_3, BPO_4, SiO_2, TiO_2, ZrO_2, Nb_2O_5, and Ta_2O_5 inhibit crystallization. Common nucleating agents, such as TiO_2, ZrO_2, MgF_2, CaF_2 and Pt were ineffective in these phosphate glasses. Crystallization of AlP_3O_9 is surface-nucleated and progresses from the surface to the interior.

The 1100 °C crystallized AlP_3O_9 is characterized by micrometre-thick, elongated columnar or lamellar AlP_3O_9 crystals with $AlPO_4$ at intergranular regions. AlF_3-doped AlP_3O_9, crystallized at 900 °C to AlP_3O_9 and $AlPO_4$, has a grain size of $\ll 0.5$ μm. Crystallization at 1000–1100 °C produces 0.5–2 μm $AlPO_4$ crystallites distributed in a lamellar matrix of AlP_3O_9. Li_2O–AlP_3O_9 glass-ceramics crystallized at 800–900 °C are inhomogeneous and contain coarse intergranular regions and glassy areas. The glassy phase is probably $LiPO_3$ or an Li–Al phosphate. Crystallization at 1000–1100 °C results in 2–10 μm lamellar AlP_3O_9 and 1–5 μm $AlPO_4$ grains. The AlP_3O_9 glass-ceramics have densities of ~ 2.4–$2.6\,g\,cm^{-3}$ and $K = 5.0$–5.2.

Acknowledgements

We thank A. Ferretti, S. A. Burroughs and R. W. Shiffer for assistance in sample preparation, K. G. Ewsuk, L. A. Harrison, Y.-H. Hu and R. Pryor for obtaining TMA and DTA data, M. L. Van Kavelaar and C. Davis for assistance with the scanning electron micrographs and W. R. Weber for obtaining the high-temperature X-ray data.

References

1. W. W. SHAVER and S. D. STOOKEY, *J. SAE* **66** (1958) 34.
2. G. H. BEALL, "Glass-Current Issues", edited by A. F. Wright and J. Dupuy (Martinus Nijhoff, Boston, 1985) pp. 31–48.
3. M. RAJARAM and D. E. DAY, *J. Amer. Ceram. Soc.* **69** (1986) 400.
4. M. R. REIDMEYER, M. RAJARAM and D. E. DAY, *J. Noncryst. Solids* **85** (1986) 186.
5. B. SALES, *Mater. Res. Soc. Bull.* 16 June (1987) 32.
6. Y. ABE, H. HOSONO and M. HOSOE, Phosphorus and Sulfur **30** (1987) 337.
7. A. KISHIOKA, M. HAYASHI and M. KINOSHITA, *Bull. Chem. Soc. Jpn* **49** (1976) 3032.
8. G. ZHENG, X. BAI and Y. SUN, *J. Noncryst. Solids* **80** (1986) 509.
9. G. H. BEALL, B. R. KARSTETTER and H. L. RITTLER, *J. Amer. Ceram. Soc.* **50** (4) (1967) 181.
10. G. H. BEALL and D. A. DUKE, *J. Mater. Sci.* **4** (1969) 340.
11. J. F. MACDOWELL and G. H. BEALL, *J. Amer. Ceram. Soc.* **52**(1) (1969) 17.
12. A. G. GREGORY and T. J. VEASEY, *J. Mater. Sci.* **6** (1971) 1312.
13. D. BAHAT, *ibid.* **7** (1972) 198.
14. P. W. McMILLAN, *Phys. Chem. Glasses* **17** (5) (1976) 193.
15. T. I. BARRY, L. A. LAY and R. MORRELL, *Sci. Ceram.* **8** (1978) 331.
16. G. H. BEALL and R. L. RITTLER, *Adv. Ceram.* **4** (1982) 301.
17. W. VOGEL and W. HOLAND, *ibid.* **4** (1982) 125.
18. K. KODAIRA, H. FUKUDA, S. SHIMADA and T. MATSUSHITA, *Mater. Res. Bull.* **19** (1984) 1427.
19. D. R. BRIDGE, D. HOLLAND and P. W. McMILLAN, *Glass Technol.* **26** (6) (1985) 286.
20. S. D. STOOKEY, US Pat. 2920 971, 12 January 1960.
21. D. M. MILLER, US Pat. 3926 648, 16 December 1975.
22. A. H. KUMAR, P. W. McMILLAN and R. R. TUMMALA, US Pat. 4301 324, 17 November 1981.
23. G. H. BEALL, US Pat. 4386 162, 31 May 1983.

24. G. CARL, K. NAUMANN, W. HOLAND and W. VOGEL, Ger. Pat. DD 242 216 Al, 21 January 1987.
25. W. ZDANIEWSKI, *J. Amer. Ceram. Soc.* **58** (5) (1975) 163.
26. K. WATANABE, E. GIESS and M. SHAFER, *J. Mater. Sci.* **20** (1985) 508.
27. E. R. VANCE, P. J. HAYWARD and I. M. GEORGE, *Phys. Chem. Glasses* **27** (2) (1986) 107.
28. V. MAIER and G. MULLER, *J. Amer. Ceram. Soc.* **70** (8) (1987) C-176.
29. T. KANAZAWA and M. HANDA, *Yogyo-Kyokai-Shi* **81** (4) (1973) 127.
30. T. KANAZAWA, H. KAWAZOE and M. HANDA, *ibid.* **80** (7) (1972) 263.
31. H. KAWAZOE, M. IKEDA and T. KANAZAWA, *ibid.* **82** (8) (1974) 462.
32. Y. ABE, T. ARAHORI and A. NARUSE, *J. Amer. Ceram. Soc.* **59** (11–12) (1976) 487.
33. Y. ABE and H. SAITO, *Yogyo-Kyokai-Shi* **85** (2) (1977) 45.
34. Y. ABE, *Nature* **282** (5734) (1979) 55.
35. J. A. WILDER, J. T. HEALEY and B. C. BUNKER, *Adv. Ceram.* **4** (1982) 313.
36. Y. ABE, M. HOSOE, T. KASUGA, H. ISHIKAWA, N. SHINKAI, Y. SUZUKI and J. NAKAYAMA, *J. Amer. Ceram. Soc.* **65** (11) (1982) C-189.
37. Y. ABE, T. KASUGA, H. HOSONO and K. DE GROOT, *ibid.* **67** (7) (1984) C-142.
38. S. KIHARA, A. WATANABE and Y. ABE, *ibid.* **67** (6) (1984) C-100.
39. P. R. CARPENTER, M. CAMPBELL, R. D. RAWLINGS and P. S. ROGERS, *J. Mater. Sci. Lett.* **5** (1986) 1309.
40. H. HOSONO, Y. SHIMIZU, H. OHSATO and Y. ABE, *ibid.* **6** (1987) 394.
41. Y. ABE, *Topics in Phosphorus Chem.* **11** (1983) 19.
42. A. KISHIOKA, *Bull. Chem. Soc. Jpn* **52** (1979) 1637.
43. C. L. QUACKENBUSH and A. KOLBECK, *Bull. Amer. Soc.* **56** (1977) 789.
44. R. M. KLEIN, A. G. KOLBECK and C. L. QUACKENBUSH, *J. Amer. Ceram. Soc.* **57** (2) (1978) 199.
45. J. F. MACDOWELL and L. E. WILSON, US Pat. 3519 445, 7 July 1970.
46. V. E. GALANT and L. N. URUSOVSKAYA, *Zh. Prikl. Khim.* **60** (1987) 2259.
47. G. T. PETROVSKII, V. E. GALANT and L. N. URUSOVSKAYA, *Dokl. Akad. Nauk. SSSR* **257** (1981) 374.
48. F. J. GONZALEZ and J. W. HALLORAN, *J. Amer. Ceram. Soc.* **63** (1980) 599.
49. D. EHRT, C. JAEGER and W. VOGEL, *Wiss. Z. Friedrich Schiller Univ. Jena Naturwiss. Reihe* **36** (1987) 867.
50. P. W. McMILLAN, "Glass-Ceramics" (Academic Press, London, 1964) pp. 24–25, 91.
51. L. D. PYE, H. J. STEVENS and W. C. LACOURSE, "Introduction to Glass Science" (Plenum Press, New York, 1972) pp. 12–14.
52. F. YVOIRE, *Bull. Soc. Chim.* **1962** (1962) 1237.
53. B. WINKHAUS, *Neues Jb. Mineral. Abh.* **83** (1951) 1.
54. A. F. WRIGHT and A. J. LEADBETTER, *Phil. Mag.* **31** (1975) 1391.
55. ASTM Card 31-27.
56. R. C. L. MOONEY, *Acta Cryst.* **9** (1956) 728.
57. O. FLORKE, *Z. Krist.* **125** (1967) 134.
58. O. FLORKE, *Science of Ceramics* **3** (1967) 13.
59. W. R. BECK, *J. Amer. Ceram. Soc.* **32** (4) (1949) 147.
60. F. A. HUMMEL, *J. Amer. Ceram. Soc.* **32** (10) (1949) 320.
61. E. C. SHAFER and R. ROY, *Z. Physik. Chemie (Neue Folge)* **11** (1957) 30.
62. W. F. HORN and F. A. HUMMEL, *Trans. Brit. Ceram. Soc.* **77** (5) (1978) 158; **79** (1980) 109.
63. E. STEGER, *Z. Anorg. Allgem. Chem.* **294** (1958) 1.
64. Y. S. BOBOVICH, *Opt. Spectrosc.* **13** (1962) 274.
65. C. HAIYAN and G. FUXI, *J. Chin. Silicate Soc.* **14** (1986) 123.
66. V. C. FARMER, "The Infrared Spectra of Minerals" (1974) pp. 383–422, 493.
67. W. VOGEL, "The Chemistry of Glass" (American Ceramic Society, Columbus, 1985) pp. 212–253.

Received 15 October 1990
and accepted 25 March 1991